Structure
Article

Structure of the Human Obesity Receptor Leptin-Binding Domain Reveals the Mechanism of Leptin Antagonism by a Monoclonal Antibody

Byron Carpenter,[1,4] Glyn R. Hemsworth,[2] Zida Wu,[3] Mabrouka Maamra,[1] Christian J. Strasburger,[3] Richard J. Ross,[1,*] and Peter J. Artymiuk[2,*]
[1]Academic Unit of Diabetes, Endocrinology and Reproduction, Department of Human Metabolism, University of Sheffield, Sheffield S10 2JF, UK
[2]Krebs Institute, Department of Molecular Biology and Biotechnology, University of Sheffield, Sheffield S10 2TN, UK
[3]Division of Endocrinology, Campus Charité Mitte, Schumannstrasse 20/21, 10117 Berlin, Germany
[4]Present address: MRC Laboratory of Molecular Biology, Hills Road, Cambridge CB2 0QH, UK
*Correspondence: r.j.ross@sheffield.ac.uk (R.J.R.), p.artymiuk@sheffield.ac.uk (P.J.A.)
DOI 10.1016/j.str.2012.01.019

SUMMARY

Leptin regulates energy homeostasis, fertility, and the immune system, making it an important drug target. However, due to a complete lack of structural data for the obesity receptor (ObR), leptin's mechanism of receptor activation remains poorly understood. We have crystallized the Fab fragment of a leptin-blocking monoclonal antibody (9F8), both in its uncomplexed state and bound to the leptin-binding domain (LBD) of human ObR. We describe the structure of the LBD-9F8 Fab complex and the conformational changes in 9F8 associated with LBD binding. A molecular model of the putative leptin-LBD complex reveals that 9F8 Fab blocks leptin binding through only a small (10%) overlap in their binding sites, and that leptin binding is likely to involve an induced fit mechanism. This crystal structure of the leptin-binding domain of the obesity receptor will facilitate the design of therapeutics to modulate leptin signaling.

INTRODUCTION

Leptin, the product of the obese (*OB*) gene, regulates energy homeostasis, fertility, and the immune system, making it an important drug target (Considine et al., 1996; Lord et al., 1998). Leptin therapy has proved successful at inducing weight loss in rare cases of congenital leptin deficiency (Farooqi et al., 1999) and correcting the metabolic abnormalities in patients with severe lipodystrophy (Oral et al., 2002). Despite the disappointing results of leptin treatment in simple obesity (Mantzoros and Flier, 2000), combination therapy with leptin and other weight regulating drugs can induce and maintain weight loss in some patients (Chan et al., 2009; Roth et al., 2008). Leptin-antagonist therapy may also have a role in the treatment of immune-mediated disorders. Leptin is permissive to a Th1 mediated immune response (Lord et al., 1998) and blockade of leptin, in animal models, imparts resistance to antigen-induced arthritis (Busso et al., 2002), multiple sclerosis (Matarese et al., 2001a; Matarese et al., 2001b), atherosclerosis (Schäfer et al., 2004), and certain types of breast cancer (Cleary et al., 2004). Thus, there is a need to develop both leptin agonists and antagonists; however, a complete lack of structural data for the obesity receptor (ObR) and its complex with leptin has been a major obstacle in their design.

The extracellular domain of ObR is composed of: an N-terminal cytokine receptor homology domain (CRH-1); an immunoglobulin-like (Ig) domain; a second CRH domain (CRH-2), also referred to as the leptin-binding domain (LBD); and two Fibronectin type III (FNIII) domains (Haniu et al., 1998). ObR shares greatest sequence homology, as well as similar extracellular domain size and organization, with the granulocyte colony stimulating factor (GCSF) receptor and glycoprotein 130 (gp130) (Haniu et al., 1998). LBD forms a high-affinity 1:1 ratio complex with leptin in solution, but does not form the 2:1 ratio complex associated with the small cytokine receptors, such as the growth hormone receptor (GHR) (Sandowski et al., 2002). The 1:1 ratio interaction occurs through leptin's binding site II, and can be blocked by mutations within this region (Iserentant et al., 2005; Niv-Spector et al., 2005b; Peelman et al., 2004; Sandowski et al., 2002). Mutations within the Ig domain of ObR and binding site III of leptin have been shown to inhibit signal transduction without disrupting receptor binding (Niv-Spector et al., 2005a; Peelman et al., 2004, 2006). This indicates that the leptin-signaling complex forms a crossover arrangement between two leptin-ObR complexes, as observed for the GCSF receptor (Tamada et al., 2006). Mutagenesis and functional studies by one group also suggest a role for leptin's putative binding site I (Peelman et al., 2004, 2006; Zabeau et al., 2004), and a model involving four ObR chains clustering around two leptin molecules, akin to the IL-6/gp130/IL-6α-receptor signaling complex, has been proposed (Peelman et al., 2006). However, the exact position of leptin's binding site I is the subject of debate (Niv-Spector et al., 2005a; Peelman et al., 2006), and it is unclear if site I is an absolute requirement for signaling.

ObR displays additional characteristics that mean, in some ways, its mechanism of signaling is likely to differ from that of

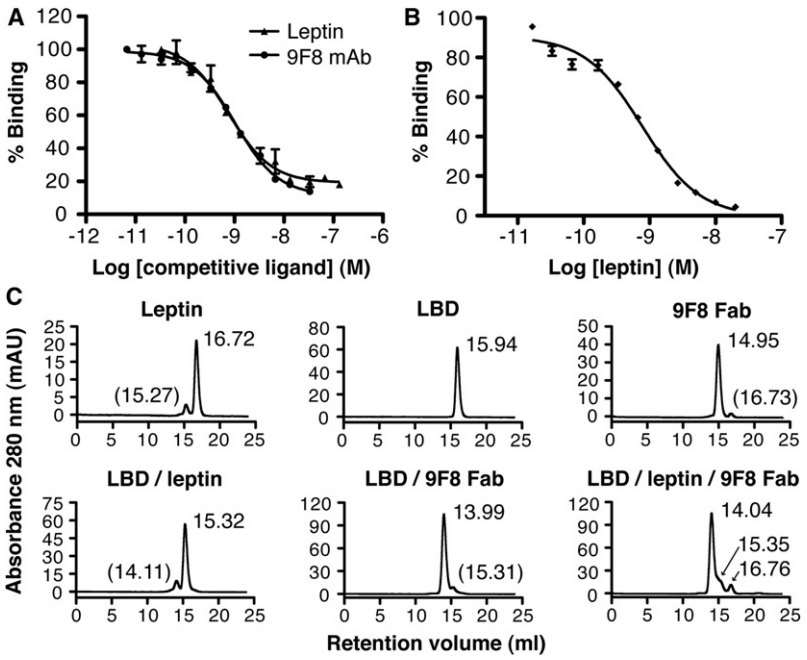

Figure 1. Analysis of Leptin and 9F8 Binding to ObR

(A) Competitive binding of leptin and 9F8 to ObR. The binding of leptin-biotin to the full-length extracellular domain of ObR was measured in the presence of either 9F8 mAb or unlabeled leptin. The IC_{50} for leptin and 9F8 mAb binding to ObR are approximately 0.76 nM and 1.0 nM, respectively (data shown are from a single experiment, and error bars represent the mean of duplicate samples).

(B) The affinity of leptin binding to recombinant LBD was calculated by competitive binding assay (data shown represent the mean of three independent experiments, and error bars indicate the standard deviation between data sets). The IC50 of leptin binding to LBD is 0.78 ± 0.05 nM (SD).

(C) Gel filtration analysis of leptin and 9F8 Fab binding to LBD. Leptin, LBD, and 9F8 Fab each resolve as a single predominant peak with retention volumes of 16.72, 15.94, and 14.95 ml, respectively (peaks shown in parentheses represent contaminants in the protein preparations). 1:1 molar ratio mixtures of LBD/leptin and LBD/9F8 Fab resolve with retention volumes of 15.32 and 13.99 ml, respectively. A 1:1:1 molar ratio mixture of all three proteins resolves as a predominant peak with a retention volume of 14.04 ml, which relates well to the LBD-9F8 Fab complex (13.99 ml). The shoulder peak (approximately 15.35 ml) is likely to contain both free 9F8 Fab (14.95 ml) and the LBD-leptin complex (15.32 ml). Significantly, no peak with a retention volume lower than 14.04 ml was present, demonstrating that leptin and 9F8 Fab cannot simultaneously bind to LBD.

GCSF and IL-6. First, ObR contains an additional CRH domain at its N terminus, which is not present in GCSF or gp130. The role of this domain is poorly understood, but there is some evidence to suggest that it enhances leptin signaling levels (Zabeau et al., 2004), and thus may play a role in complex formation. Second, ObR is known to dimerize in a ligand-independent fashion both on the cell surface and in solution (Couturier and Jockers, 2003; Devos et al., 1997; Nakashima et al., 1997; White et al., 1997), possibly through disulphide bridges between its membrane-proximal FNIII domains (Zabeau et al., 2005). However, it is currently unclear how these dimers are arranged and whether leptin binding causes formation of the crossover complex within a single dimer or between a pair of dimers. Thus, crystal structures of both ObR and its complex with leptin are greatly needed to elucidate the full mechanism of leptin signaling.

Despite extensive crystallization trials of LBD, alone or in complex with leptin, obtaining crystals has proved difficult. We previously identified a mouse monoclonal antibody (9F8), which acts as an antagonist of leptin signaling (Fazeli et al., 2006). Initially we crystallized 9F8 in its uncomplexed state and solved its crystal structure at 2.3 Å resolution. We then used Fab-mediated crystallization to solve the structure of 9F8 Fab complexed with LBD at 1.95 Å resolution. Herein, we describe the structure of the LBD-9F8 Fab complex, and the changes induced in 9F8 Fab by LBD binding. We also constructed and characterized a molecular docking model of the leptin-LBD complex, which reveals the mechanism by which 9F8 Fab antagonizes leptin signaling.

RESULTS

Characterization of Leptin and 9F8 Fab Binding to LBD and ObR

It has previously been shown that 9F8 mAb can displace leptin from the full-length extracellular domain of ObR (Fazeli et al., 2006). However, the mechanism of displacement was unclear and it was not known if 9F8 Fab bound within the isolated LBD. Therefore, we designed a number of experiments to further characterize 9F8 and leptin binding to LBD and ObR. First, we used a competitive binding assay to confirm that 9F8 mAb can efficiently displace leptin from the full-length extracellular domain of ObR (Fazeli et al., 2006). Leptin was efficiently displaced from ObR by 9F8; IC_{50} values were calculated to be approximately 0.76 nM for leptin and 1.0 nM for 9F8 (Figure 1A). Next, we refolded and purified the isolated LBD from *Escherichia coli* and used a competitive binding assay to ensure recombinant LBD was functional (Figure 1B). We calculated the IC_{50} of leptin binding to recombinant LBD to be 0.78 ± 0.05 nM, which compares well with previous reports in the literature (Kamikubo et al., 2008; Niv-Spector et al., 2005b; Sandowski et al., 2002). Finally, we used analytical gel filtration to show that 9F8 Fab binds within the isolated LBD and that leptin and 9F8 Fab cannot simultaneously bind to LBD (Figure 1C).

Structure of Uncomplexed 9F8 Fab

The asymmetric unit of the crystal contains a single 9F8 Fab molecule (Figure 2A). The structure of 9F8 Fab is typical of that of most antibody Fab fragments, although it contains a number

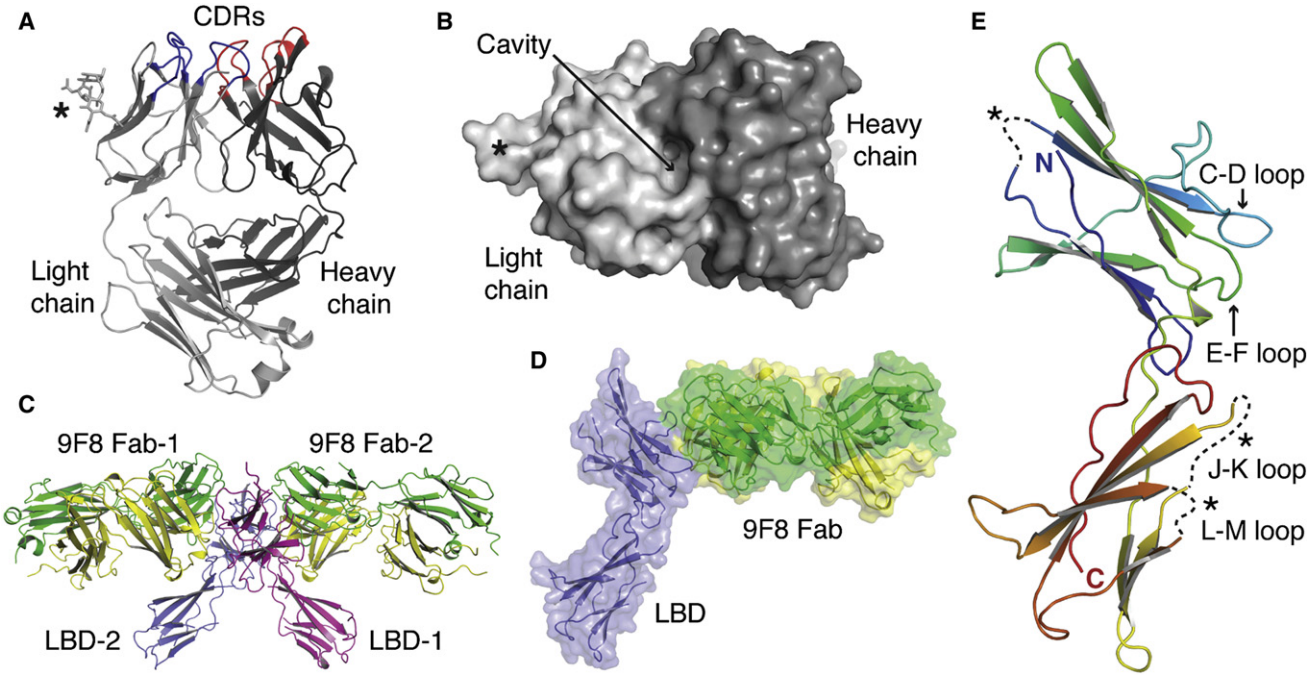

Figure 2. Crystal Structures of 9F8 Fab and the LBD-9F8 Fab Complex

(A) Ribbon representation of the 9F8 Fab. The CDRs from the light chain (light gray) and heavy chain (dark gray) are colored blue and red, respectively. The glycosylation of Asn-22 of the light chain is shown as sticks and marked by an asterisk.

(B) Surface representation of the CDR regions of 9F8 Fab. The deep cavity at the interface between the light and heavy chains is clearly visible; the glycosylation of Asn-22 of the light chain is marked by an asterisk.

(C) Ribbon representation of the two copies of the LBD-9F8 Fab complex in the asymmetric unit. The two LBD molecules are colored blue and magenta, the 9F8 Fab molecules are colored yellow (heavy chain) and green (light chain).

(D) A single copy of the LBD-9F8 Fab complex showing that 9F8 Fab binds to the N-terminal subdomain of LBD.

(E) Secondary structural elements of LBD colored by rainbow: N terminus, blue; C terminus, red. Key loops, which are discussed in the text, are labeled; unmodeled loops are indicated by dashed lines and marked with an asterisk. Figures made using Pymol (http://www.pymol.org).

See also Figure S1.

of interesting features. First, 9F8 is glycosylated at Asn-22 of the light chain, close to the complementarity determining regions (CDRs). In the uncomplexed structure good density is observed for some of the sugar moiety, due to its involvement in crystal lattice contacts, and thus one fucose residue and two N-acetylglucosamine sugars could be modeled (Figure 2A). In the LBD-9F8 Fab structure (see below) this region was devoid of crystal contacts and a single N-acetylglucosamine sugar residue was modeled in one copy of the light chain only (chain F). Despite its proximity to the CDRs, the glycosylation is not required for binding to ObR (Fazeli et al., 2006). Second, 9F8 contains a deep cavity within the surface of the CDRs, at the interface between the heavy and light chains (Figure 2B), the importance of which, with respect to receptor binding, is discussed below.

Structure of the LBD-9F8 Fab Complex

The asymmetric unit of the crystal (Figure 2C) contains two copies of the LBD-9F8 Fab complex (Figure 2D), which interact through a major interface between the LBD molecules. The LBD molecules are arranged in a cross-shaped complex (Figure 2C; Figure S1A available online), which is reminiscent of the erythropoietin (EPO) receptor ligand-independent dimer (PDB: 1ERN) (Livnah et al., 1999; Figure S1A). However, the buried surface area of the LBD interface is only 700 Å^2 and involves minimal direct interactions, which is consistent with the observation that LBD does not dimerize in solution. Therefore, we conclude that the interface is most likely to be a crystal packing interaction, but cannot rule out a low-affinity interaction through this site in the full-length, membrane-bound receptor.

LBD is a β sheet rich protein composed of two subdomains, both of which adopt a fibronectin type III fold (Figures 2E and 3). The overall electron density for the LBD molecules is very good, but several loop regions, 39 residues in total, could not be satisfactorily modeled due to poor electron density (Figure S1B). Three disulphide bonds are observed within the N-terminal subdomain, between residues 436–447, 473–528, and 488–498 (Figure S1C). The two cysteine residues located within the C-terminal subdomain (Cys-604 and Cys-613) do not interact with one another. Cys-604 is exposed on the surface of the protein and is cysteinylated, which is most likely a consequence of using cysteine as a reducing agent while refolding LBD (Figure S1C). Interestingly, the cysteinylation is involved in a major crystal lattice contact between LBD and the Fab heavy chain from a neighboring complex. Mutation of the two free cysteine residues (C604A/C613A) improved the yield of purified LBD 6-fold with no loss in affinity for leptin (data not shown). However, the mutant failed to crystallize in complex with 9F8 Fab, demonstrating that the cysteinylation was integral for lattice formation in this particular

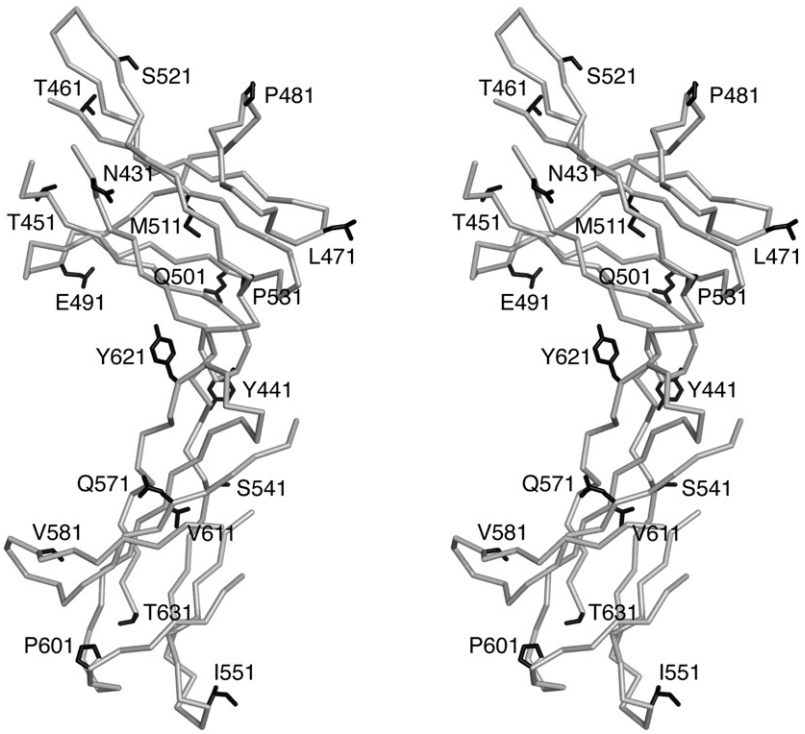

Figure 3. Stereo Diagram of LBD Structure
Ribbon representation of LBD (light gray); every tenth amino acid side chain is shown as sticks and colored black.

crystal form. The C-terminal domain of LBD also contains the highly conserved WSXWS motif, which forms the basis of a π-cation stack involving Arg-573, Trp-583, Arg-612, and Lys-614 (Figure S1C). A global alignment using the program DALI (Holm et al., 2008) indicated that LBD is most structurally similar to the EPO receptor (PDB: 1EBP) (Livnah et al., 1996).

LBD-9F8 Fab Interaction

The LBD-9F8 Fab interface has a total buried surface area of 1,500 Å^2. All of the direct polar contacts, a total of eight hydrogen bonds and three salt bridges (Table 1), are formed between LBD and the Fab heavy chain (CDRs: H1, H2, and H3) (Figure 4A). The interface also contains an extensive network of van der Waals interactions involving both the heavy chain (CDRs: H1, H2, and H3) and light chain (CDRs: L2 and L3) of 9F8 Fab (Table 1). The interacting surfaces of LBD and 9F8 Fab display opposite electrostatic potentials: the LBD surface carries a net positive charge, contrasting with the negatively charged CDRs of 9F8 Fab. The electrostatic component of the interface is reflected by the formation of three salt bridges between the proteins (see Figure 4A and Table 1). The interacting surfaces of LBD and 9F8 Fab also display a high degree of shape complementarity (Figure 4B). Most striking is the insertion of Ile-482 of LBD into the deep cavity on the surface of 9F8 (Figure 4C). Ile-482 is positioned less than 4 Å from six residues that line the cavity (Trp-54 and His-103 from the heavy chain; His-53, Trp-94, Tyr-96, and Leu-98 from the light chain), demonstrating the highly specific nature of this interaction. The degree of shape complementarity was quantified using the program SC (Lawrence and Colman, 1993). The S_c score of the LBD-9F8 Fab interface was 0.75 ± 0.0 (average of the two interfaces in the AU), which is well above the range of most antibody-antigen interfaces (S_c = 0.64-0.68), and most similar to highly conserved protein/protein-inhibitor complexes (S_c = 0.71–0.76) (Lawrence and Colman, 1993).

Conformational Changes in 9F8 Fab upon LBD Binding

The availability of refined crystal structures of 9F8 in both complexed and uncomplexed states (Table 2) allows a global alignment of these two forms of the Fab fragment. This results in an rmsd of 0.99 ± 0.09 Å (average of two Fab molecules in the LBD-9F8 Fab structure). This deviation primarily results from a major structural rearrangement within the elbow region of each Fab chain. It has been reported that an increase in the Fab elbow angle (flexion) can be induced by antigen binding, resulting from the variable regions of the heavy and light chain moving independently to one another (Teplyakov et al., 2011). However in the present case, a lateral rotation (approximately 8°) occurs in the elbow region, which does not affect the flexion angle. Furthermore, superposition of just the variable regions of the complexed and uncomplexed Fab molecules results in an rmsd of only 0.51 ± 0.00 Å (average of two Fab molecules in the LBD-9F8 Fab structure), demonstrating that the variable regions do not move in relation to one another. Therefore we conclude that the distortion in the elbow region of 9F8 Fab is not induced by LBD binding, and is most likely a result of crystal packing constraints.

Superposition of the variable domains permits an assessment of the specific changes induced by LBD binding. Only minor conformational changes (less than 1 Å) are seen in most of the CDRs, including side chain atoms, with the exception of CDR H3 (Figure 4D). CDR H3 is involved in 6 of the 11 polar contacts in the interface (Table 1) and undergoes a maximum shift of 2.5 Å upon LBD binding (Figure 4D). Within this loop, His-103 undergoes a rotamer change allowing it to interact with Glu-484 of LBD; Glu-104, which is disordered in uncomplexed 9F8, becomes highly ordered and interacts with His-467, Ser-469, and Ser-470 of LBD. The movement of CDR H3 also creates a small pocket, which accommodates Ser-470 of LBD (Figure 4B). A movement of 0.8 Å is also observed in CDR L3 upon complexation, which is induced by a rotamer shift in His-93 (Figure 4D). In its new position His-93 forms 35 van der Waals contacts with residues from the reorientated CDR H3 (His-100, His-103, Glu-104 and Thr-105), stabilizing its LBD-interacting conformation. Asn-95 from CDR L3 also undergoes a rotamer change, relieving a potential steric clash with Pro-481, and allowing it to form three van der Waals contacts with this residue. The reconfiguration of CDRs L3 and H3 also causes a 2.7 Å contraction of the surface cavity of 9F8 Fab, into which Ile-482 of LBD inserts (Figures 4C and 4D).

Table 1. Summary of Close Contacts between LBD and 9F8 Fab

Polar Interactions				
LBD Residue (Chain B)	Bond Type	Distance (Å)	9F8 Fab Residue (Heavy Chain D)	CDR
Arg-465 (NH2)	H-bond	3.1	Tyr-60 (OH)	H2
His-467 (NE2)	Salt bridge	2.8	Glu-104 (OE2)	H3
Arg-468 (O)	H-bond	2.9	His-103 (N)	H3
Arg-468 (NH1)	H-bond	3.3	Asp-33 (O)	H1
Arg-468 (NH1)	Salt bridge	3.1	Asp-34 (OD1)	H1
Arg-468 (NH2)	Salt bridge	3.9	Asp-34 (OD1)	H1
Ser-469 (OG)	H-bond	2.6	Glu-104 (OE1)	H3
Ser-470 (N)	H-bond	2.9	Glu-104 (OE1)	H3
Ser-470 (OG)	H-bond	2.9	Asp-101 (O)	H3
Glu-484 (OE1)	H-bond	2.8	Gly-56 (N)	H2
Glu-484 (OE2)	H-bond	2.7	His-103 (NE2)	H3
Van der Waals Interactions				
LBD Residue (Chain B)	9F8 Fab Residue	9F8 Fab Chain	CDR	Number of Contacts
His-467	His-103	Heavy (chain D)	H3	5
His-467	Glu-104	Heavy (chain D)	H3	5
Arg-468	His-103	Heavy (chain D)	H3	9
Arg-468	Gly-102	Heavy (chain D)	H3	6
Arg-468	Asp-34	Heavy (chain D)	H1	3
Ser-469	Glu-104	Heavy (chain D)	H3	9
Ser-470	Asp-101	Heavy (chain D)	H3	9
Leu-471	Leu-52	Light (chain F)	L2	4
Leu-471	Asn-55	Light (chain F)	L2	3
Pro-481	Asn-95	Light (chain F)	L3	6
Pro-481	Trp-94	Light (chain F)	L3	9
Ile-482	Trp-94	Light (chain F)	L3	3
Ile-482	His-93	Light (chain F)	L3	4
Glu-484	Trp-54	Heavy (chain D)	H2	5
Glu-484	His-103	Heavy (chain D)	H3	4
Phe-504	Asp-33	Heavy (chain D)	H1	4

Hydrogen bonds and salt bridges were calculated using PISA (Krissinel and Henrick, 2007). Hydrogen bonds are defined as interactions exhibiting the necessary geometry with contact distances of 3.3 Å or less. Salt bridges are defined as interactions exhibiting the necessary geometry, electrostatic charge, and protonation state with contact distances of 4.0 Å or less. Van der Waals interactions were calculated using the CONTACT function of CCP4i (Potterton et al., 2003) and are defined as interactions with contact distances of 4.0 Å or less, excluding hydrogen bonds and salt bridges. Only residues that form three or more van der Waals contacts are shown.

Evidence against the Involvement of LBD in Disulphide Dimerization of ObR

It has been suggested that cysteine residues within LBD mediate ligand-independent dimerization of ObR on the cell surface (Zabeau et al., 2005). LBD contains two unpaired cysteine residues: Cys-613 is totally buried in the core of the protein, whereas Cys-604 is located in a solvent exposed position on the surface of LBD. Thus, Cys-604 initially appeared to be a good candidate to be involved in disulphide dimerization of ObR. However, alignment of LBD with the structure of the full gp130 ectodomain (PDB: 3L5H) (Xu et al., 2010) revealed that Gly-339 from the downstream FNIII domain of gp130 is positioned only 4.3 Å away from Cys-604 of LBD (Figure 5). Primary structure alignment of these receptors shows that Gly-339 from gp130 aligns perfectly with Cys-674 of ObR. Therefore, it is most likely that an intramolecular disulphide bond forms between Cys-604 and Cys-674 of ObR, indicating cysteine residues within LBD are not responsible for dimerization of ObR. Hence, other conserved cysteine residues within the FNIII domains of ObR (Haniu et al., 1998) may be involved in receptor dimerization, and warrant further investigation.

A Model for Leptin Binding to LBD

We generated a rigid body docking model of the leptin-LBD complex using the GRAMM-X server (Tovchigrechko and Vakser, 2006). Two loops (J-K and L-M loops) within the C-terminal subdomain of LBD have fragmented electron density, presumably due to conformational flexibility, and are omitted from the final structure. However, indicative loops were modeled in order to reconstruct the molecular surface for docking experiments (Figure S2). We modeled the J-K loop in both LBD molecules from the asymmetric unit, but no consensus could be reached for its orientation between the two chains. In fact, the

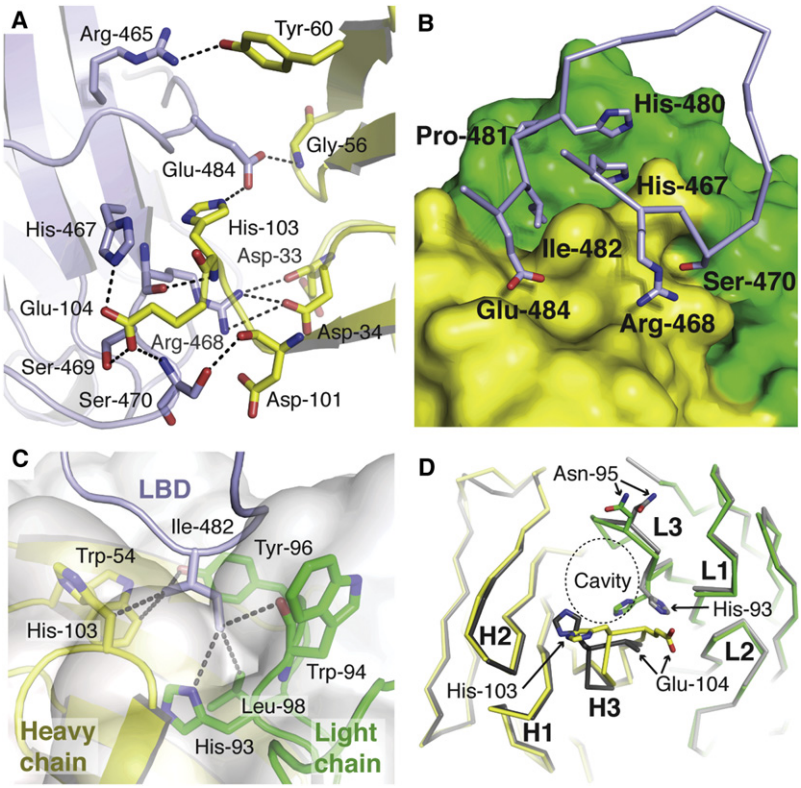

Figure 4. Interaction of 9F8 Fab with LBD

(A) Polar interactions between the 9F8 Fab heavy chain (yellow) and LBD (light blue).

(B) Illustration of the high degree of shape complementarity between the C-D loop of LBD (light blue) and the molecular surface of the 9F8 Fab light chain (green) and heavy chain (yellow).

(C) Positioning of LBD residue Ile-482 (light blue) in a deep cavity within the solvent accessible surface of 9F8 Fab (white), at the interface between the Fab heavy (yellow) and light (green) chains. The closest contact between Ile-482 and each Fab residue is displayed, and are all within the range 3.5–3.9 Å.

(D) Structural changes in 9F8 Fab induced by LBD binding. The light and heavy chains of uncomplexed 9F8 Fab are colored light gray and dark gray respectively; the light and heavy chains of complexed 9F8 Fab are colored green and yellow, respectively. CDR H3 undergoes a 2.5 Å movement upon complexation (measured between CA of His-103); CDR L3 undergoes a 0.8 Å movement upon complexation (measured between CA of Asn-95); the surface cavity of 9F8 contracts by 2.7 Å upon complexation (measured between CA of Asn-95 and His-103). Side chains whose rotamers change upon receptor binding are shown as sticks and discussed in the text.

best fit achieved in the two LBD molecules indicated two different conformations of the loop, particularly in the region around Phe-563 (Figures 6A and 6B; Figure S2): in one molecule (chain A) Phe-563 appears to be located in a solvent exposed position; in the other molecule (chain B) Phe-563 is largely buried in the core of the protein. Defining this observation as two distinct orientations of the J-K loop is speculative, and it is more likely that a large number of conformations exist under physiological conditions. However these two putative configurations provided a good basis for docking simulations, and allowed us to investigate the importance of this loop in leptin binding.

Docking experiments were also undertaken to investigate the existence of the putative leptin binding site I. However, interpretation of these results was more difficult than the site II simulations for a number of reasons: the putative interaction is low affinity (Sandowski et al., 2002); only a small amount of mutagenesis data is available for the proposed interface (Peelman et al., 2004); and the surface of LBD predicted to be involved in the site I interface overlaps with that involved in site II interactions. Therefore, we were unable to reach any conclusions about the existence of the putative binding site I through docking experiments.

In the docking experiment directed toward leptin binding site II, one of the highest scoring output models (Figure 6C) showed remarkable similarity to both the GCSF/GCSF receptor (PDB: 2D9Q) (Tamada et al., 2006) and IL-6/gp130 (PDB: 1P9M) (Boulanger et al., 2003) complexes. The rmsd between the complexes is approximately 3 Å in both cases, which is similar to the rmsd when the individual proteins are superimposed. The predicted area of the leptin/LBD interface is approximately 1,500 Å^2, which also compares closely with that of GCSF/GCSFR (1,400 Å^2) and IL-6/gp130 (1,700 Å^2). Most significantly, this model correlates with results from mutagenesis studies (Iserentant et al., 2005; Niv-Spector et al., 2005b; Peelman et al., 2004) as described below.

The hydrophobic E-F loop of LBD contains six residues (Phe-500, Ile-503, Phe-504, Leu-505, Leu-506, Ser-507) (Figure 6B) which, when mutated to alanine, dramatically reduce leptin binding affinity and signal transduction (Iserentant et al., 2005; Niv-Spector et al., 2005b). Interestingly, two of these residues (Phe-500 and Ile-503) have their side chains almost totally buried in the core of the protein, and do not interact with leptin. Leu-505 and Leu-506 align with the hydrophobic cavity between helices 1 and 3 of leptin, a region previously identified as important for receptor binding (Iserentant et al., 2005), forming van der Waals interactions with Leu-13 and Leu-86 (Figure 6D). This network of van der Waals interactions also involves residues belonging to the SSLY motif of LBD. Leu-471 and Tyr-472 form extensive van der Waals interactions with Val-6, Leu-86, and Val-89 of leptin (Figure 6D). Unexpectedly, Phe-504 of LBD does not align with the hydrophobic cavity, instead it is surrounded by polar residues from leptin (Asn-78, Glu-81, and Asn-82). However, Phe-504 may play a significant role in coordinating Arg-468 through a π-cation stacking interaction (Figure 6C), positioning it well to interact with Asn-82 and Asp-85 of leptin; mutation of any of these three residues dramatically decreases binding affinity (Niv-Spector et al., 2005b; Peelman et al., 2004).

The Flexible J-K Loop of LBD Mediates Contacts with Leptin

Contacts between the C-terminal subdomain of LBD and leptin appear to be predominantly mediated by the flexible J-K loop. In both docking models (based on LBD chains A and B) Phe-563, Pro-564, Glu-565, and Asn-566 from the J-K loop are positioned parallel to helix 1 of leptin. Mutation of Glu-565 and

Table 2. X-Ray Crystallographic Data Processing and Refinement Statistics

Data Collection Statistics	9F8 Fab	LBD-9F8 Fab
Space group	C2	$P2_12_12_1$
Cell dimensions		
a (Å)	139.2	89.8
b (Å)	40.0	118.8
c (Å)	105.1	171.3
α, β, γ (°)	90,128.0,90	90,90,90
Solvent (%)[a]	46.7	59.6
Resolution range (Å)	37–2.26 (2.38–2.26)	49–1.95 (2.00–1.95)
Completeness (%)	97.1 (82.0)	99.9 (99.9)
Unique reflections	21,142	127,050
Wilson B-factor (Å^2)	36.3	22.1
Multiplicity	2.6 (2.5)	7.2 (7.4)
I/σ (%)	11.7 (3.3)	15.9 (3.8)
R_{merge} (%)[b]	6.4 (27.7)	7.4 (55.6)
Data refinement statistics	9F8 Fab	LBD-9F8 Fab
R_{cryst} (%)[c]	19.0	17.1
R_{free} (%)[d]	25.9	21.1
Number of atoms (nonhydrogen)		
Total	3,362	10,514
Nonprotein	138	1,014
Water	91	851
Acetate	4	24
Carbohydrate	38	14
Ethylene glycol	—	124
Sodium	—	1
Sulfate	5	—
Rmsd		
Bond angles (°)	1.90	1.8
Bond lengths (Å^2)	0.019	0.023
Average B-factors (Å^2)		
Main-chain atoms	35.9	35.4
Side-chain atoms	37.0	40.7
Water	32.2	42.5
All atoms	36.9	38.4
Ramachandran statistics (%)		
Most favored regions	95.6	97.2
Disallowed regions	1.2	0.3

Values in parentheses represent the highest-resolution shell.
[a]Solvent content estimated from Matthews coefficient.
[b]$R_{merge} = \Sigma|I - < I > |/\Sigma I$, where I is the integrated intensity of a given reflection.
[c]$R_{work} = \Sigma||F(obs)| - |F(calc)||/\Sigma|F(obs)|$ for the 95% of the reflection data used in refinement.
[d]$R_{free} = \Sigma||F(obs)| - |F(calc)||/\Sigma|F(obs)|$ for the remaining 5% of the reflection data excluded from the refinement.

Asn-566 causes a reduction in the level of signal transduction (30% and 50%, respectively) (Iserentant et al., 2005), and mutation of Phe-563 causes an 18-fold decrease in binding affinity (Niv-Spector et al., 2005b). We discussed previously that the

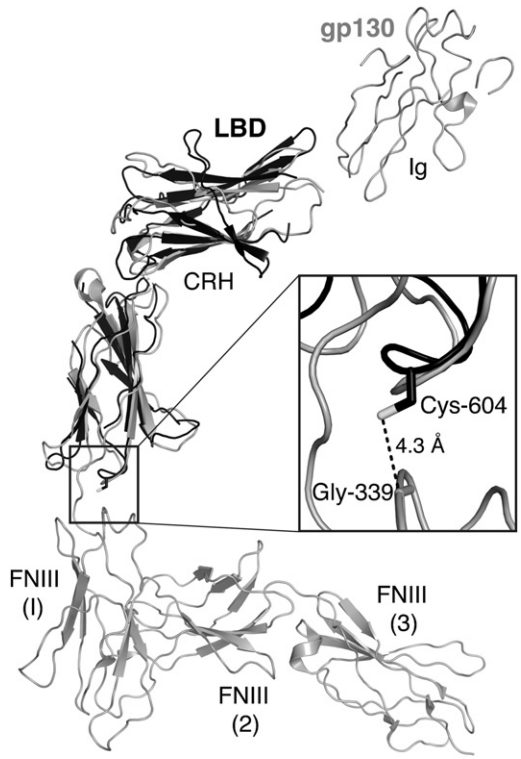

Figure 5. Proposed Interdomain Disulphide Bond in ObR
Superposition of LBD (black) on the full-length extracellular domain of gp130 (gray) (PDB: 3L5H) (Xu et al., 2010), showing the position of the proposed interdomain disulphide bond. In the superimposition Cys-604 of LBD is positioned 4.3 Å from Gly-339 of gp130 (inset). In a primary structure alignment between the two receptors Cys-674 of ObR aligns precisely with Gly-339 of gp130. Therefore, we predict that an intramolecular, interdomain disulphide bond is likely to form at this position in ObR.

J-K loop of LBD was modeled in two different conformations (Figure 6A; Figure S2). In LBD chain A Phe-563 was modeled in a solvent exposed position: in this docking model Phe-563 forms extensive van der Waals contacts with polar residues from leptin (Thr-16, Thr-19, Arg-20, and Asp-23), but it lacks a specific hydrophobic or aromatic binding partner. In LBD chain B Phe-563 was modeled in a buried position, and does not interact with leptin. Therefore our docking model agrees with published mutagenesis data, which suggests leptin interacts with the J-K loop (Iserentant et al., 2005; Niv-Spector et al., 2005b). However, it is unclear whether Phe-563 forms direct contacts with leptin or instead stabilizes the correct orientation of the J-K loop to allow leptin binding.

The Leptin and 9F8 Fab Binding Sites Are Predicted to Partially Overlap

We used the leptin-LBD model to investigate the mechanism by which 9F8 Fab neutralizes leptin signaling. Superposition of the LBD-leptin model onto the LBD-9F8 Fab structure indicates a small but significant overlap between the observed 9F8 Fab, and the predicted leptin-binding sites (Figure 6E). The common overlap region consists of approximately 80 Å^2 of the LBD surface that would be buried in both interfaces: this relates to only about 10% of the total surface of LBD that is buried in either

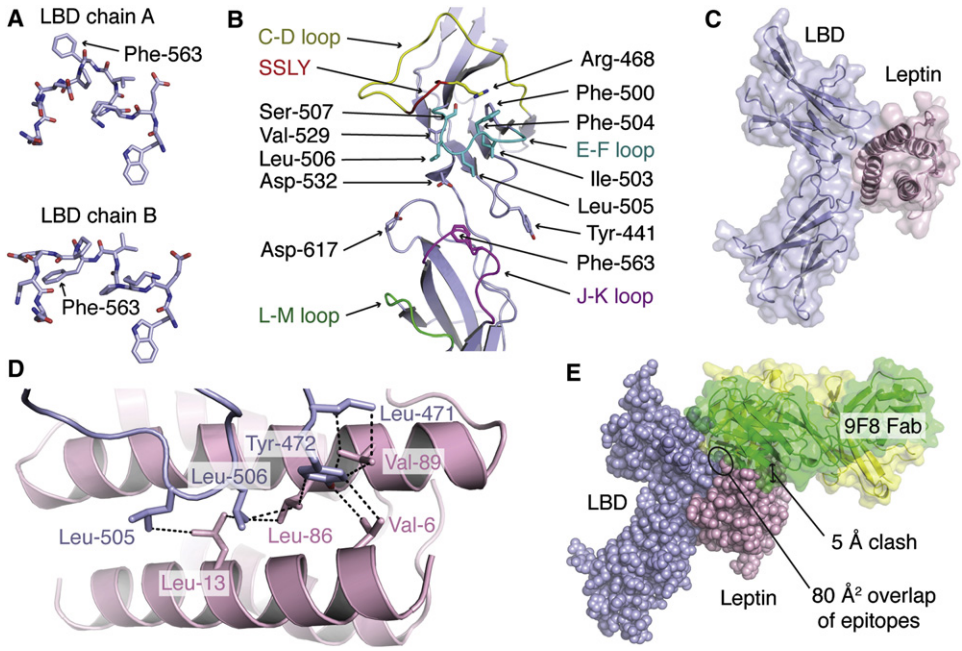

Figure 6. A Model of Leptin Binding to LBD

(A) Differences in the flexible J-K loop modeled in the two LBD molecules. Phe-563 appears to adopt a solvent exposed position in chain A, but is largely buried within the core of LBD in chain B.

(B) LBD residues implicated in leptin binding by mutagenesis studies are shown as sticks. Important loops, which are discussed in the text are colored: C-D loop, yellow; E-F loop, cyan; J-K loop, magenta; L-M loop, green. The SSLY motif, which is located within the C-D loop, is colored red.

(C) A putative model of the leptin-LBD complex (light blue and pink, respectively) was generated by rigid body docking experiments.

(D) Hydrophobic and aromatic residues from the C-D loop (471–472) and E-F loop (505–506) of LBD (light blue) aligned with the hydrophobic cavity between helices 1 and 3 of leptin (pink). All contacts shown are less than 4.2 Å.

(E) Superposition of 9F8 Fab (yellow/green) with the LBD-leptin model (light blue and pink, respectively). The 9F8 Fab and leptin binding-sites overlap by approximately 80 Å^2 on the surface of LBD. A sterically forbidden clash of 5 Å is predicted between leptin and the 9F8 Fab light chain if they were to bind LBD simultaneously.

See also Figure S2.

the 9F8 Fab (800 Å^2) or predicted leptin (750 Å^2) interfaces. The overlap region involves six LBD residues (Arg-468, Ser-469, Ser-470, Leu-471, Pro-502, and Phe-504). All of these residues form direct contacts (less than 4 Å) with 9F8 Fab (Table 1) and five are predicted to form direct interactions with leptin (Arg-468, Ser-470, Leu-471, Pro-502, and Phe-504). In addition to the surface overlap, a sterically forbidden overlap of main chain atoms by approximately 5 Å is predicted to occur between leptin and the 9F8 Fab light chain if they were to bind LBD simultaneously (Figure 6E).

DISCUSSION

We have crystallized 9F8 Fab in its uncomplexed state and used Fab-mediated crystallization to solve the structure of the LBD-9F8 Fab complex. The structures have allowed us to characterize the changes induced in 9F8 by LBD binding. Our findings also provide valuable insight into the mechanism of leptin binding to LBD and the mechanism of 9F8 antagonism of leptin signaling.

To date, crystallization of the isolated LBD or a leptin-LBD complex has proved difficult. Although there are numerous possible reasons for this, a major contributing factor is likely to be the presence of several flexible loops within LBD, which limit the surface area amenable to crystal contact formation. Fab-mediated crystallization is a powerful technique used to improve the crystallization properties of challenging proteins by stabilizing dynamic regions, increasing the hydrophilic surface area available for crystal lattice formation, and masking unfavorable regions of the protein surface (Koide, 2009). Here, it was successfully employed to crystallize LBD, and in future the use of nonneutralizing antibodies, that bind either leptin or LBD, may facilitate crystallization of the leptin-LBD complex.

The structures of 9F8 Fab in both its uncomplexed and receptor-bound forms give valuable insight into its mechanism of antigen recognition. Electrostatic interactions, shape complementarity and conformational rearrangement all play an important role in antigen binding. Receptor binding induces minor changes in the Fab structure, which are limited to mainly small rearrangements in individual CDRs, the degree of which is consistent with other antibody-antigen complexes (Davies and Cohen, 1996). Interestingly CDR H3, which is involved in over half of the polar contacts in the interface, undergoes a larger (2.5 Å) movement upon receptor binding. Rearrangement of CDR H3 is coupled to a rotamer shift in His-93 (CDR L3), which appears to stabilize CDR H3 in its receptor binding conformation. The rearrangements in CDRs H3 and L3 also result in a 2.7 Å contraction of the 9F8 surface cavity into which Ile-482

of LBD tightly fits. Therefore antigen binding involves a limited induced fit mechanism, which is likely to contribute to the high degree of shape complementarity observed in the interface.

In order to characterize the leptin-binding site of LBD, we generated a model of the leptin-LBD complex using the crystal structures of both leptin (PDB: 1AX8) (Zhang et al., 1997) and LBD. Several groups have reported models of the leptin-LBD complex based on homology models of LBD (Hiroike et al., 2000; Iserentant et al., 2005; Sandowski et al., 2002). The overall arrangement of the leptin-LBD complex in our model appears similar to these previously published homology models, but many of the specific interactions reported differ significantly. In particular, our model predicts an important role for Tyr-472 of LBD in leptin binding, which has not been identified from previous homology models. Interestingly, our model predicts that the main site of leptin binding within the C-terminal subdomain of LBD is likely to be the J-K loop, which the crystal structure of LBD revealed to be highly flexible. This provides strong evidence that leptin binding involves an induced fit mechanism.

We analyzed the corresponding regions from uncomplexed cytokine receptor structures to determine if flexible loops are a common feature of cytokine binding. Currently the only structures available for class-I cytokine receptors in their monomeric, uncomplexed states are: the IL-6α receptor (PDB: 1N26) (Varghese et al., 2002); gp130 (PDB: 1BQU and 3L5H) (Bravo et al., 1998; Xu et al., 2010); and GHR (PDB: 2AEW) (Brown et al., 2005). GHR is the only receptor to show significant flexibility in its equivalent of the J-K loop (Brown et al., 2005). Superposition of the uncomplexed structure with that of the growth hormone-bound receptor (PDB: 1A22) (Clackson et al., 1998) shows that the loop becomes ordered upon ligand binding. Therefore, an induced fit mechanism of ligand binding may be of wider significance within the cytokine receptor family.

We used analytical gel filtration and competitive binding assays to demonstrate that leptin and 9F8 Fab cannot simultaneously bind to LBD. Molecular modeling of the leptin-LBD complex revealed that the 9F8 Fab and leptin binding sites partially overlap. Thus, in respect to the isolated LBD, the antagonist action of 9F8 Fab is most likely to result from direct competition between 9F8 Fab and leptin binding. In vivo, inhibition of ObR dimerization or higher order clustering may represent a secondary mechanism of antagonism, particularly with regard to the full antibody; allosteric inhibition of ObR has recently been demonstrated using cameloid antibodies directed against its membrane proximal FNIII domains (Zabeau et al., 2012). Superposition of the LBD-9F8 Fab complex onto the structure of the GCSF and IL-6 signaling complexes demonstrates that 9F8 Fab would neither disrupt formation of the crossover complex, nor prevent binding of an additional receptor to leptin's putative binding site I region. However, because the exact arrangement of the ObR signaling complex is unknown, a secondary mechanism of 9F8 antagonism in vivo cannot be discounted.

The observation that 9F8 Fab blocks leptin binding through only a 10% overlap in their epitopes is a surprising finding, which has implications for the assignment of functional sites in target proteins solely on the basis of antibody modulation of function. It also suggests that when creating therapeutic neutralizing antibodies a much wider range of potential peptide epitopes should be considered than those restricted to the major functional sites.

What implications does our study have for the design of novel leptin-modulating therapeutics? First, we have shown that 9F8 binds within the isolated LBD, with a similar affinity to leptin, and that their binding is mutually exclusive. Second, we have crystallized 9F8 Fab in both its uncomplexed and receptor-bound forms, and characterized the changes in 9F8 induced by LBD binding. Therefore, 9F8 mAb is a good template for structure-based design of a potent leptin antagonist with strong therapeutic potential. Finally, because we predict that the epitopes of leptin and 9F8 Fab overlap by only 10%, 9F8 Fab represents a useful tool to mediate cocrystallization of LBD with potential peptide or small molecule drug candidates.

In summary, we have crystallized 9F8 Fab both in its uncomplexed state and in complex with LBD, and characterized the changes induced in 9F8 Fab caused by receptor binding. We constructed and characterized a putative model of the leptin-LBD complex, and proposed an induced fit mechanism for leptin binding. We also used the leptin-LBD model to propose that 9F8 Fab antagonizes leptin binding through a partial overlap in their binding sites. To our knowledge, this is the first report of a crystal structure for any part of the obesity receptor and will facilitate the design of therapeutics to modulate leptin signaling.

EXPERIMENTAL PROCEDURES

LBD Production and Analysis

LBD (residues 428–635 of human ObR) was expressed, refolded and purified essentially as described previously (Sandowski et al., 2002). Competitive binding assays were performed in ELISA format: ObR and LBD were captured using nonneutralizing antibodies and detected using biotinylated leptin or 9F8. Full details are provided in the Supplemental Experimental Procedures.

9F8 Fab Production

The identification and characterization of 9F8 mAb has been described previously (Fazeli et al., 2006). 9F8 mAb was expressed in the monoclonal hybridoma cell line and was purified by protein A affinity chromatography (Pierce). Fab fragments were prepared by digestion of the purified mAb with immobilized papain (Pierce) at 37°C for 5 hr. Fab fragments were isolated by negative purification on a protein A column, and further purified by gel filtration.

Crystallization and Structure Solution of 9F8 Fab

Crystals of 9F8 Fab were grown by hanging-drop vapor diffusion against crystallization buffer (0.2 M ammonium sulfate, 0.1 M sodium acetate [pH 4.6], 25% PEG-4000) at a protein concentration of 10 mg/ml. Crystals grew to maximum size in 2 weeks at 17°C. Crystals were cryoprotected in crystallization buffer containing 20% glycerol for 1 min, before freezing in a dry nitrogen stream at 100 K.

Diffraction data were collected in-house using a Micromax 007 source and MAR345 detector. Data were indexed using MOSFLM (Leslie, 2006) and scaled using SCALA (Evans, 1993). Data processing was performed using the CCP4 program package (Potterton et al., 2003); full statistics are shown in Table 2. The structure was solved by molecular replacement using PHASER (McCoy et al., 2005), using chains A and D of the pdb deposition 1CIC (Bentley et al., 1990) as models for the heavy and light chains, respectively. Refinement was performed by the maximum likelihood method using REFMAC (Murshudov et al., 1997), with manual rebuilding using COOT (Emsley and Cowtan, 2004).

Crystallization and Structure Solution of the LBD-9F8 Fab Complex

LBD and 9F8 Fab were mixed in a 1:1 stochiometric ratio, incubated overnight at 4°C and purified by gel filtration. Crystals were grown by hanging-drop vapor diffusion against crystallization buffer (100 mM sodium acetate pH 4.6, 150 mM unbuffered sodium acetate, 5% PEG-4000), at a protein concentration of 7.5 mg/ml. Crystals grew to maximum size in 2–3 weeks at 8°C. Crystals were cryoprotected in crystallization buffer containing 30% ethylene glycol for 1 min, before freezing in a dry nitrogen stream at 100 K.

Diffraction data were collected on beamline I02 at Diamond Synchrotron (Oxfordshire, UK). Data were indexed using MOSFLM (Leslie, 2006) and scaled using SCALA (Evans, 1993). Data processing was performed using the CCP4 program package (Potterton et al., 2003); full statistics are shown in Table 2. The structure was phased using PHASER (McCoy et al., 2005), by molecular replacement with the structure of 9F8 Fab. The amino acid sequence of LBD was fitted using ARP-WARP (Cohen et al., 2008). Refinement was performed by the maximum likelihood method using REFMAC (Murshudov et al., 1997), with manual rebuilding using COOT (Emsley and Cowtan, 2004). The final models were validated using MOLPROBITY (Davis et al., 2007), and further details are provided in the Supplemental Experimental Procedures section.

Protein-Protein Docking Experiments

Docking was performed using the GRAMM-X protein-protein docking server (Tovchigrechko and Vakser, 2006). The J-K and L-M loops of LBD had fragmented electron density, and thus they are omitted from the final structure. However, indicative loops were modeled in order to reconstruct the molecular surface for docking experiments (Figure S2). Different conformations of the J-K loop were modeled in LBD chains A and B, and are discussed in the text. Docking simulations were conducted using both LBD molecules.

In order to limit the search area to the putative binding sites of both LBD and leptin (PDB: 1AX8) (Zhang et al., 1997) a small number of key residues were specified to be involved in the interface. Three LBD residues (Phe-504, Leu-505, and Leu-506) and two leptin residues (Arg-20 and Gln-75) were selected based on: data from mutagenesis studies, their central location within the putative binding sites, and their solvent exposed position on the protein surface. The final models were subjected to 20 cycles of energy minimization, using the GROMOS96 implementation of the Swiss-pdb viewer (Guex and Peitsch, 1997), to resolve a number of small stereochemical clashes. Docking models are provided in Supplemental Data File 1 online.

ACCESSION NUMBERS

Atomic coordinates and structure factors of 9F8 Fab and the LBD-9F8 Fab complex have been deposited in the Protein Data Bank, http://www.pdb.org (PDB code 3VG0 and 3V6O, respectively).

SUPPLEMENTAL INFORMATION

Supplemental Information includes Supplemental Experimental Procedures and two figures and can be found with this article online at doi:10.1016/j.str.2012.01.019.

ACKNOWLEDGMENTS

Z.W., C.J.S., and R.J.R. have a granted patent in the US and Europe on the use of the 9F8 antibody for the treatment of autoimmune disease, and R.J.R., P.J.A., and B.C. have a patent application on the use of the 9F8 epitopes in the development of therapeutic antibodies. However, neither of these is currently being exploited commercially. We thank Diamond Light Source for access to beamline I02 (BAG MX300) that contributed to the results presented here. We thank Svetlana Sedelnikova for assistance with analytical gel filtration. Monoclonal antibody Fab Fragments were prepared by the Antibody Resource Centre (Sheffield, UK). B.C. was in receipt of an Medical Research Council PhD studentship. G.R.H. was in receipt of a Biotechnology and Biological Sciences Research Council PhD studentship. G.R.H. and M.M. crystallized 9F8 Fab. G.R.H. solved the structure of 9F8 Fab. B.C. cloned, expressed and purified LBD and leptin, and crystallized the LBD-9F8 Fab complex; B.C. and G.R.H. solved the LBD-9F8 Fab structure; B.C., Z.W., and C.J.S. carried out functional studies; Z.W. and C.J.S. provided new reagents; P.J.A. and R.J.R. directed the research; B.C., P.J.A., and R.J.R. wrote the paper.

Received: October 31, 2011
Revised: January 13, 2012
Accepted: January 22, 2012
Published: March 6, 2012

REFERENCES

Bentley, G.A., Boulot, G., Riottot, M.M., and Poljak, R.J. (1990). Three-dimensional structure of an idiotope-anti-idiotope complex. Nature *348*, 254–257.

Boulanger, M.J., Chow, D.C., Brevnova, E.E., and Garcia, K.C. (2003). Hexameric structure and assembly of the interleukin-6/IL-6 alpha-receptor/gp130 complex. Science *300*, 2101–2104.

Bravo, J., Staunton, D., Heath, J.K., and Jones, E.Y. (1998). Crystal structure of a cytokine-binding region of gp130. EMBO J. *17*, 1665–1674.

Brown, R.J., Adams, J.J., Pelekanos, R.A., Wan, Y., McKinstry, W.J., Palethorpe, K., Seeber, R.M., Monks, T.A., Eidne, K.A., Parker, M.W., and Waters, M.J. (2005). Model for growth hormone receptor activation based on subunit rotation within a receptor dimer. Nat. Struct. Mol. Biol. *12*, 814–821.

Busso, N., So, A., Chobaz-Péclat, V., Morard, C., Martinez-Soria, E., Talabot-Ayer, D., and Gabay, C. (2002). Leptin signaling deficiency impairs humoral and cellular immune responses and attenuates experimental arthritis. J. Immunol. *168*, 875–882.

Chan, J.L., Roth, J.D., and Weyer, C. (2009). It takes two to tango: combined amylin/leptin agonism as a potential approach to obesity drug development. J. Investig. Med. *57*, 777–783.

Clackson, T., Ultsch, M.H., Wells, J.A., and de Vos, A.M. (1998). Structural and functional analysis of the 1:1 growth hormone:receptor complex reveals the molecular basis for receptor affinity. J. Mol. Biol. *277*, 1111–1128.

Cleary, M.P., Juneja, S.C., Phillips, F.C., Hu, X., Grande, J.P., and Maihle, N.J. (2004). Leptin receptor-deficient MMTV-TGF-alpha/Lepr(db)Lepr(db) female mice do not develop oncogene-induced mammary tumors. Exp. Biol. Med. *229*, 182–193.

Cohen, S.X., Ben Jelloul, M., Long, F., Vagin, A., Knipscheer, P., Lebbink, J., Sixma, T.K., Lamzin, V.S., Murshudov, G.N., and Perrakis, A. (2008). ARP/wARP and molecular replacement: the next generation. Acta Crystallogr. D Biol. Crystallogr. *64*, 49–60.

Considine, R.V., Sinha, M.K., Heiman, M.L., Kriauciunas, A., Stephens, T.W., Nyce, M.R., Ohannesian, J.P., Marco, C.C., McKee, L.J., Bauer, T.L., et al. (1996). Serum immunoreactive leptin concentrations in normal-weight and obese humans. N. Engl. J. Med. *334*, 292–295.

Couturier, C., and Jockers, R. (2003). Activation of the leptin receptor by a ligand-induced conformational change of constitutive receptor dimers. J. Biol. Chem. *278*, 26604–26611.

Davies, D.R., and Cohen, G.H. (1996). Interactions of protein antigens with antibodies. Proc. Natl. Acad. Sci. USA *93*, 7–12.

Davis, I.W., Leaver-Fay, A., Chen, V.B., Block, J.N., Kapral, G.J., Wang, X., Murray, L.W., Arendall, W.B., 3rd, Snoeyink, J., Richardson, J.S., and Richardson, D.C. (2007). MolProbity: all-atom contacts and structure validation for proteins and nucleic acids. Nucleic Acids Res. *35* (Web Server issue), W375–W383.

Devos, R., Guisez, Y., Van der Heyden, J., White, D.W., Kalai, M., Fountoulakis, M., and Plaetinck, G. (1997). Ligand-independent dimerization of the extracellular domain of the leptin receptor and determination of the stoichiometry of leptin binding. J. Biol. Chem. *272*, 18304–18310.

Emsley, P., and Cowtan, K. (2004). Coot: model-building tools for molecular graphics. Acta Crystallogr. D Biol. Crystallogr. *60*, 2126–2132.

Evans, P.R. (1993). Data reduction. Proceedings of the CCP4 Study Weekend 1993, on Data Collection & Processing, 114–122.

Farooqi, I.S., Jebb, S.A., Langmack, G., Lawrence, E., Cheetham, C.H., Prentice, A.M., Hughes, I.A., McCamish, M.A., and O'Rahilly, S. (1999). Effects of recombinant leptin therapy in a child with congenital leptin deficiency. N. Engl. J. Med. *341*, 879–884.

Fazeli, M., Zarkesh-Esfahani, H., Wu, Z., Maamra, M., Bidlingmaier, M., Pockley, A.G., Watson, P., Matarese, G., Strasburger, C.J., and Ross, R.J. (2006). Identification of a monoclonal antibody against the leptin receptor that acts as an antagonist and blocks human monocyte and T cell activation. J. Immunol. Methods *312*, 190–200.

Guex, N., and Peitsch, M.C. (1997). SWISS-MODEL and the Swiss-PdbViewer: an environment for comparative protein modeling. Electrophoresis *18*, 2714–2723.

Haniu, M., Arakawa, T., Bures, E.J., Young, Y., Hui, J.O., Rohde, M.F., Welcher, A.A., and Horan, T. (1998). Human leptin receptor. Determination of disulfide structure and N-glycosylation sites of the extracellular domain. J. Biol. Chem. *273*, 28691–28699.

Hiroike, T., Higo, J., Jingami, H., and Toh, H. (2000). Homology modeling of human leptin/leptin receptor complex. Biochem. Biophys. Res. Commun. *275*, 154–158.

Holm, L., Kääriäinen, S., Rosenström, P., and Schenkel, A. (2008). Searching protein structure databases with DaliLite v.3. Bioinformatics *24*, 2780–2781.

Iserentant, H., Peelman, F., Defeau, D., Vandekerckhove, J., Zabeau, L., and Tavernier, J. (2005). Mapping of the interface between leptin and the leptin receptor CRH2 domain. J. Cell Sci. *118*, 2519–2527.

Kamikubo, Y., Dellas, C., Loskutoff, D.J., Quigley, J.P., and Ruggeri, Z.M. (2008). Contribution of leptin receptor N-linked glycans to leptin binding. Biochem. J. *410*, 595–604.

Koide, S. (2009). Engineering of recombinant crystallization chaperones. Curr. Opin. Struct. Biol. *19*, 449–457.

Krissinel, E., and Henrick, K. (2007). Inference of macromolecular assemblies from crystalline state. J. Mol. Biol. *372*, 774–797.

Lawrence, M.C., and Colman, P.M. (1993). Shape complementarity at protein/protein interfaces. J. Mol. Biol. *234*, 946–950.

Leslie, A.G. (2006). The integration of macromolecular diffraction data. Acta Crystallogr. D Biol. Crystallogr. *62*, 48–57.

Livnah, O., Stura, E.A., Johnson, D.L., Middleton, S.A., Mulcahy, L.S., Wrighton, N.C., Dower, W.J., Jolliffe, L.K., and Wilson, I.A. (1996). Functional mimicry of a protein hormone by a peptide agonist: the EPO receptor complex at 2.8 A. Science *273*, 464–471.

Livnah, O., Stura, E.A., Middleton, S.A., Johnson, D.L., Jolliffe, L.K., and Wilson, I.A. (1999). Crystallographic evidence for preformed dimers of erythropoietin receptor before ligand activation. Science *283*, 987–990.

Lord, G.M., Matarese, G., Howard, J.K., Baker, R.J., Bloom, S.R., and Lechler, R.I. (1998). Leptin modulates the T-cell immune response and reverses starvation-induced immunosuppression. Nature *394*, 897–901.

Mantzoros, C.S., and Flier, J.S. (2000). Editorial: leptin as a therapeutic agent—trials and tribulations. J. Clin. Endocrinol. Metab. *85*, 4000–4002.

Matarese, G., Di Giacomo, A., Sanna, V., Lord, G.M., Howard, J.K., Di Tuoro, A., Bloom, S.R., Lechler, R.I., Zappacosta, S., and Fontana, S. (2001a). Requirement for leptin in the induction and progression of autoimmune encephalomyelitis. J. Immunol. *166*, 5909–5916.

Matarese, G., Sanna, V., Di Giacomo, A., Lord, G.M., Howard, J.K., Bloom, S.R., Lechler, R.I., Fontana, S., and Zappacosta, S. (2001b). Leptin potentiates experimental autoimmune encephalomyelitis in SJL female mice and confers susceptibility to males. Eur. J. Immunol. *31*, 1324–1332.

McCoy, A.J., Grosse-Kunstleve, R.W., Storoni, L.C., and Read, R.J. (2005). Likelihood-enhanced fast translation functions. Acta Crystallogr. D Biol. Crystallogr. *61*, 458–464.

Murshudov, G.N., Vagin, A.A., and Dodson, E.J. (1997). Refinement of macromolecular structures by the maximum-likelihood method. Acta Crystallogr. D Biol. Crystallogr. *53*, 240–255.

Nakashima, K., Narazaki, M., and Taga, T. (1997). Leptin receptor (OB-R) oligomerizes with itself but not with its closely related cytokine signal transducer gp130. FEBS Lett. *403*, 79–82.

Niv-Spector, L., Gonen-Berger, D., Gourdou, I., Biener, E., Gussakovsky, E.E., Benomar, Y., Ramanujan, K.V., Taouis, M., Herman, B., Callebaut, I., et al. (2005a). Identification of the hydrophobic strand in the A-B loop of leptin as major binding site III: implications for large-scale preparation of potent recombinant human and ovine leptin antagonists. Biochem. J. *391*, 221–230.

Niv-Spector, L., Raver, N., Friedman-Einat, M., Grosclaude, J., Gussakovsky, E.E., Livnah, O., and Gertler, A. (2005b). Mapping leptin-interacting sites in recombinant leptin-binding domain (LBD) subcloned from chicken leptin receptor. Biochem. J. *390*, 475–484.

Oral, E.A., Simha, V., Ruiz, E., Andewelt, A., Premkumar, A., Snell, P., Wagner, A.J., DePaoli, A.M., Reitman, M.L., Taylor, S.I., et al. (2002). Leptin-replacement therapy for lipodystrophy. N. Engl. J. Med. *346*, 570–578.

Peelman, F., Van Beneden, K., Zabeau, L., Iserentant, H., Ulrichts, P., Defeau, D., Verhee, A., Catteeuw, D., Elewaut, D., and Tavernier, J. (2004). Mapping of the leptin binding sites and design of a leptin antagonist. J. Biol. Chem. *279*, 41038–41046.

Peelman, F., Iserentant, H., De Smet, A.S., Vandekerckhove, J., Zabeau, L., and Tavernier, J. (2006). Mapping of binding site III in the leptin receptor and modeling of a hexameric leptin.leptin receptor complex. J. Biol. Chem. *281*, 15496–15504.

Potterton, E., Briggs, P., Turkenburg, M., and Dodson, E. (2003). A graphical user interface to the CCP4 program suite. Acta Crystallogr. D Biol. Crystallogr. *59*, 1131–1137.

Roth, J.D., Roland, B.L., Cole, R.L., Trevaskis, J.L., Weyer, C., Koda, J.E., Anderson, C.M., Parkes, D.G., and Baron, A.D. (2008). Leptin responsiveness restored by amylin agonism in diet-induced obesity: evidence from nonclinical and clinical studies. Proc. Natl. Acad. Sci. USA *105*, 7257–7262.

Sandowski, Y., Raver, N., Gussakovsky, E.E., Shochat, S., Dym, O., Livnah, O., Rubinstein, M., Krishna, R., and Gertler, A. (2002). Subcloning, expression, purification, and characterization of recombinant human leptin-binding domain. J. Biol. Chem. *277*, 46304–46309.

Schäfer, K., Halle, M., Goeschen, C., Dellas, C., Pynn, M., Loskutoff, D.J., and Konstantinides, S. (2004). Leptin promotes vascular remodeling and neointimal growth in mice. Arterioscler. Thromb. Vasc. Biol. *24*, 112–117.

Tamada, T., Honjo, E., Maeda, Y., Okamoto, T., Ishibashi, M., Tokunaga, M., and Kuroki, R. (2006). Homodimeric cross-over structure of the human granulocyte colony-stimulating factor (GCSF) receptor signaling complex. Proc. Natl. Acad. Sci. USA *103*, 3135–3140.

Teplyakov, A., Obmolova, G., Malia, T., and Gilliland, G. (2011). Antigen recognition by antibody C836 through adjustment of V(L)/V(H) packing. Acta Crystallogr. Sect. F Struct. Biol. Cryst. Commun. *67*, 1165–1167.

Tovchigrechko, A., and Vakser, I.A. (2006). GRAMM-X public web server for protein-protein docking. Nucleic Acids Res. *34* (Web Server issue), W310–4.

Varghese, J.N., Moritz, R.L., Lou, M.Z., Van Donkelaar, A., Ji, H., Ivancic, N., Branson, K.M., Hall, N.E., and Simpson, R.J. (2002). Structure of the extracellular domains of the human interleukin-6 receptor alpha -chain. Proc. Natl. Acad. Sci. USA *99*, 15959–15964.

White, D.W., Kuropatwinski, K.K., Devos, R., Baumann, H., and Tartaglia, L.A. (1997). Leptin receptor (OB-R) signaling. Cytoplasmic domain mutational analysis and evidence for receptor homo-oligomerization. J. Biol. Chem. *272*, 4065–4071.

Xu, Y., Kershaw, N.J., Luo, C.S., Soo, P., Pocock, M.J., Czabotar, P.E., Hilton, D.J., Nicola, N.A., Garrett, T.P., and Zhang, J.G. (2010). Crystal structure of the entire ectodomain of gp130: insights into the molecular assembly of the tall cytokine receptor complexes. J. Biol. Chem. *285*, 21214–21218.

Zabeau, L., Defeau, D., Van der Heyden, J., Iserentant, H., Vandekerckhove, J., and Tavernier, J. (2004). Functional analysis of leptin receptor activation using a Janus kinase/signal transducer and activator of transcription complementation assay. Mol. Endocrinol. *18*, 150–161.

Zabeau, L., Defeau, D., Iserentant, H., Vandekerckhove, J., Peelman, F., and Tavernier, J. (2005). Leptin receptor activation depends on critical cysteine residues in its fibronectin type III subdomains. J. Biol. Chem. *280*, 22632–22640.

Zabeau, L., Verhee, A., Catteeuw, D., Faes, L., Seeuws, S., Decruy, T., Elewaut, D., Peelman, F., and Tavernier, J. (2012). Selection of non-competitive leptin antagonists using a random nanobody-based approach. Biochem. J. *441*, 425–434.

Zhang, F., Basinski, M.B., Beals, J.M., Briggs, S.L., Churgay, L.M., Clawson, D.K., DiMarchi, R.D., Furman, T.C., Hale, J.E., Hsiung, H.M., et al. (1997). Crystal structure of the obese protein leptin-E100. Nature *387*, 206–209.